iScience

Article

Evolution of tumor stress response during cytoreductive surgery for ovarian cancer

Graphical abstract

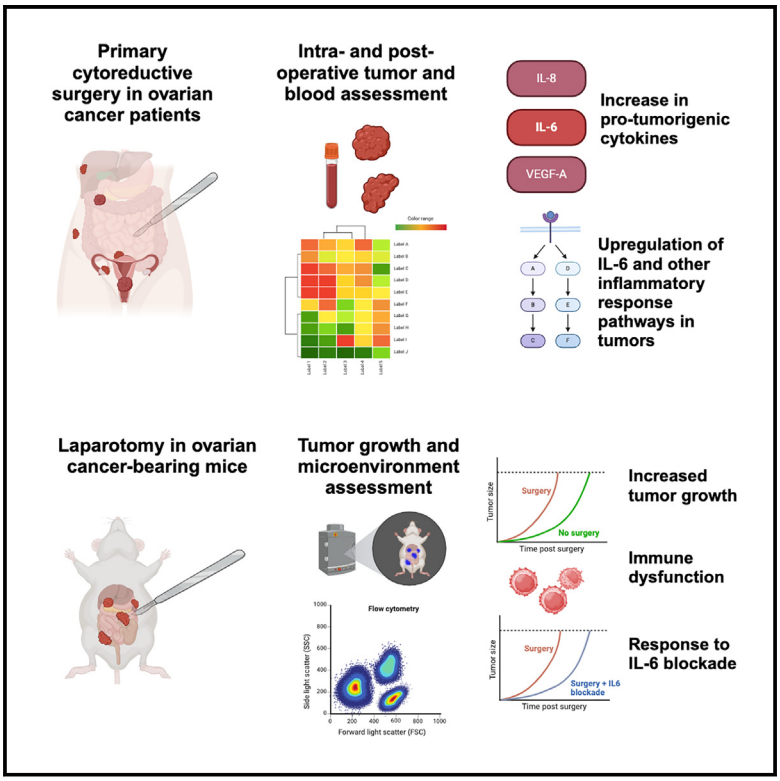

Highlights

- Timing of intraoperative tumor collection impacts tumor transcriptional profiles
- Ovarian cancer cytoreductive surgery induces intra-tumoral inflammatory response
- Surgical inflammatory response stimulates ovarian cancer growth in mouse model
- These findings generate rationale for perioperative anti-inflammatory interventions

Authors

Aaron M. Praiss, Lea A. Moukarzel, Yingjie Zhu, ..., Rui Gardner, Britta Weigelt, Dmitriy Zamarin

Correspondence

dmitriy.zamarin@mssm.edu

In brief

Cell biology; Cancer

Praiss et al., 2025, iScience *28*, 112317
May 16, 2025
https://doi.org/10.1016/j.isci.2025.112317

CellPress

iScience

CellPress
OPEN ACCESS

Article

Evolution of tumor stress response during cytoreductive surgery for ovarian cancer

Aaron M. Praiss,[1,7] Lea A. Moukarzel,[1] Yingjie Zhu,[2] Ana Leda F. Longhini,[3] Fatemeh Derakhshan,[2] Timothy Hoang,[2] Giulio Pesci,[4] Hunter Green,[2] Melih A. Ozsoy,[5] Etta Hanlon,[2] Ryan Kahn,[1] Melica Nourmoussavi Brodeur,[2] Tiffany Sia,[1] Nadeem R. Abu-Rustum,[1,5] Ginger Gardner,[1,5] Kara Long Roche,[1,5] Yukio Sonoda,[1,5] Oliver Zivanovic,[1] Dennis S. Chi,[1,5] Taha Merghoub,[4] Rui Gardner,[3] Britta Weigelt,[2] and Dmitriy Zamarin[6,8,9,*]

[1]Gynecology Service, Department of Surgery, Memorial Sloan Kettering Cancer Center, New York, NY, USA
[2]Department of Pathology and Laboratory Medicine, Memorial Sloan Kettering Cancer Center, New York, NY, USA
[3]Department of Flow Cytometry, Memorial Sloan Kettering Cancer Center, New York, NY, USA
[4]Ludwig Collaborative Laboratory, Weill Cornell Medicine, New York, NY, USA
[5]Department of OB/GYN, Weill Cornell Medical College, New York, NY, USA
[6]Precision Immunology Institute, Icahn School of Medicine at Mount Sinai, New York, NY, USA
[7]X (formerly Twitter): @AaronPraissMD
[8]X (formerly Twitter): @DmitriyZamarin
[9]Lead contact
*Correspondence: dmitriy.zamarin@mssm.edu
https://doi.org/10.1016/j.isci.2025.112317

SUMMARY

Upfront treatment for patients with advanced high-grade serous ovarian cancer (HGSOC) includes a multi-hour cytoreductive surgery. Although the procedure is necessary for maximal tumor cytoreduction, understanding of the biology of systemic and intratumoral responses induced by surgical cytoreduction is limited. Through analysis of matched tumor and normal tissues and peripheral blood collected at multiple time points during cytoreductive surgery in patients with HGSOC, we demonstrate that surgery leads to rapid induction of systemic inflammatory response and activation of inflammatory signaling in the tumor and normal tissue, with interleukin-6 emerging as a dominant inflammatory pathway. A parallel study in a syngeneic murine HGSOC model recapitulated these findings and demonstrated accelerated tumor growth in response to surgery. This study highlights the previously unappreciated impact of specimen collection timing on the tumor signaling networks and provides insights into stress pathways activated by surgery, generating rationale for perioperative therapeutic interventions to reduce protumorigenic effects.

INTRODUCTION

Ovarian cancer (OC) is one of the most lethal gynecologic malignancies in the United States, with an estimated 12,740 deaths in 2024.[1] Patients often present with advanced-stage disease due to a lack of effective screening, vague symptom onset, and peritoneal spread of the disease throughout the abdominopelvic cavity. For patients with advanced OC, the upfront treatment paradigm includes cytoreductive surgery and systemic chemotherapy with a platinum-doublet regimen. Because of the peritoneal spread of the disease, cytoreductive surgery often requires multiple hours and involves resection of the gynecologic organs and upper abdominal disease including omentum and possible splenectomy and/or bowel resection.

Although cytoreductive surgery remains necessary in the upfront treatment of advanced-stage OC, increasing evidence indicates that any surgical intervention is associated with perioperative stress that involves paracrine and neuroendocrine response; this increases proangiogenic factors, suppresses antitumor immunity, and facilitates malignant cell invasion, which ultimately has the potential to facilitate tumor growth and metastases.[2–6] In animal cancer models, Auer et al. have performed elegant studies on the impact of surgery on murine cancers,[4,5] demonstrating that surgical interventions lead to profound suppression of innate immune function (specifically natural killer [NK] cells) in the postoperative period, which correlate with increased development of metastases.[4] A variety of human clinical studies have reported accelerated growth of residual tumors after cytoreductive surgery, typically linked to increased protumorigenic cytokines and upregulation of numerous tumorigenic pathways.[7–11]

Several studies have suggested that perioperative changes in peripheral plasma cytokines may play a role in tumorigenesis.[6,12,13] Secord et al. demonstrated that postsurgical inflammatory cytokine interleukin-6 (IL-6) in plasma may predict therapeutic benefit from bevacizumab when combined with carboplatin and paclitaxel in the GOG 218 trial in patients with newly diagnosed OC.[14,15] Stone et al. assessed the impact of paraneoplastic thrombocytosis in patients with OC and demonstrated that increased levels of thrombopoietin and IL-6 fueled

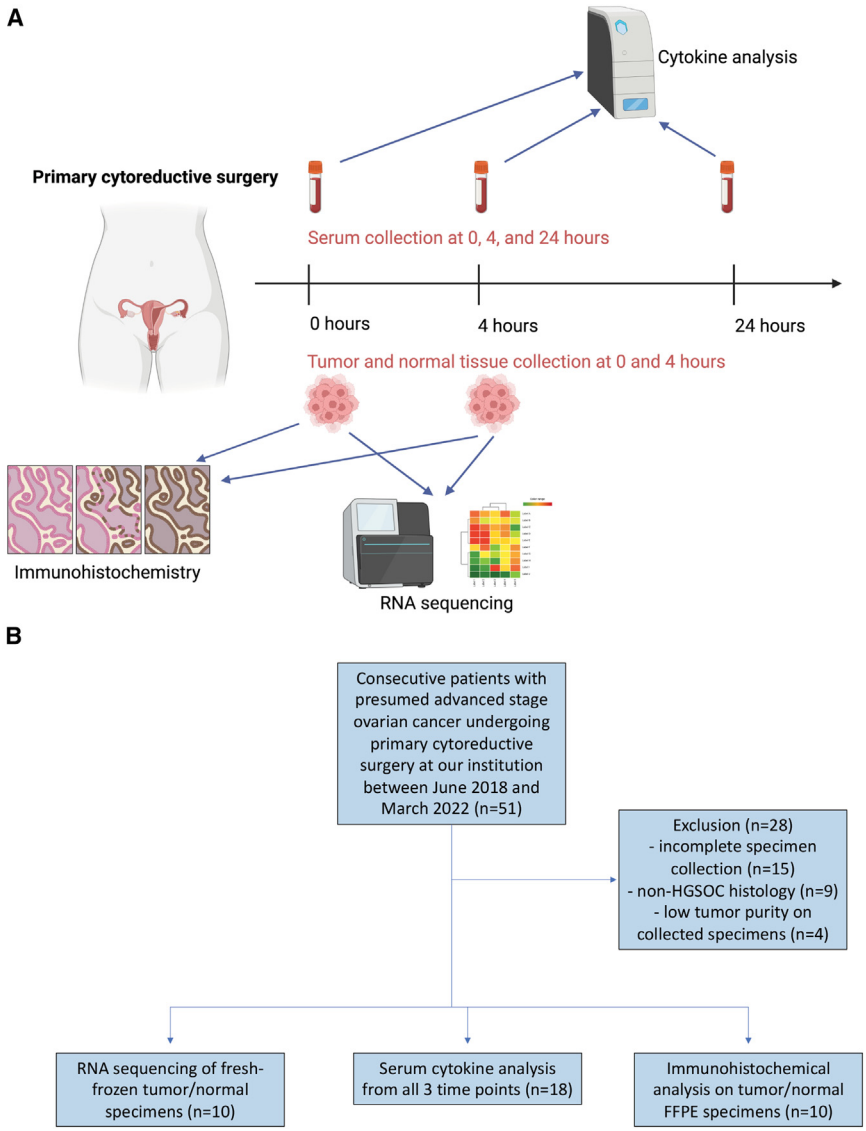

Figure 1. Methodology for human subject tissue and plasma collection and cohort selection

(A) Experimental design for human subject tumor/normal tissue and plasma collection during and after primary cytoreductive surgery for advanced-stage high-grade serous ovarian cancer.

(B) CONSORT (Consolidated Standards of Reporting Trials) flow chart of high-grade serous ovarian cancer case selection and downstream analyses. FFPE, formalin-fixed paraffin-embedded; H&E, hematoxylin and eosin; IHC, immunohistochemistry, HGSOC, high-grade serous ovarian cancer.

tumor growth.[16] Retrospective data also suggest that modulation of perioperative stress in OC through therapeutic interventions could be associated with improved outcomes. A retrospective analysis by Tseng et al. demonstrated independently associated improved progression-free and overall survival in patients with OC who received perioperative epidural anesthesia compared to those who did not.[17]

Despite these findings, translational data pertaining to the impact of surgical intervention and stress on actual tumors and normal tissues remain limited, particularly in OC. Published transcriptional profiling datasets, such as those from The Cancer Genome Atlas (TCGA) for OC and other cancers, do not take into account the exact time at which the tumor biospecimen was collected after the initial incision and the potential heterogeneity in post-resection tumor processing (e.g., time to flash freezing), which makes it impossible to study how surgery impacts tumor biology. To overcome this challenge, we took advantage of the multi-hour procedure to perform serial sampling of matched tumors and normal biospecimens, which allowed us to control for biospecimen timing, site, and post-collection processing during primary cytoreductive surgery (PCS) for high-grade serous OC (HGSOC). We performed orthogonal analyses in a genetically engineered HGSOC murine model driven by *myc* amplification and *Tp53* and *Brca1* deletion (MPB). We sought to assess the impact of laparotomy on the evolution of intratumoral and systemic inflammatory response in patients, define the impact of surgery on tumor growth and long-term tumor microenvironment in animal models, and evaluate a perioperative anti-cytokine therapeutic strategy to counter the protumorigenic stress response. Through this work, we demonstrate that surgery leads to rapid induction of systemic inflammatory response and activation of inflammatory signaling in the tumor and normal tissue, leading to accelerated tumor growth in animal models. Our study provides insights into intratumoral signaling pathways activated by surgery, generating rationale for perioperative therapeutic interventions to reduce the protumorigenic effects.

RESULTS

Surgical intervention leads to upregulation of inflammatory signaling pathways in HGSOC

Biopsies of tumor tissue and normal peritoneum were collected shortly after initial incision (TP1) and 3–4 h into the surgery (TP2). Tumor specimens were collected from the same anatomic site to minimize the potential impact of inter-site heterogeneity (Figure 1). RNA-sequencing analysis performed on HGSOC and normal specimens collected immediately after laparotomy (TP1) and 3–4 h (TP2) into cytoreductive surgery from 10 patients revealed a marked upregulation of a number of genes in both tumor and normal tissue samples (Figure 2A). Hierarchical clustering of the top upregulated genes showed that samples from the same

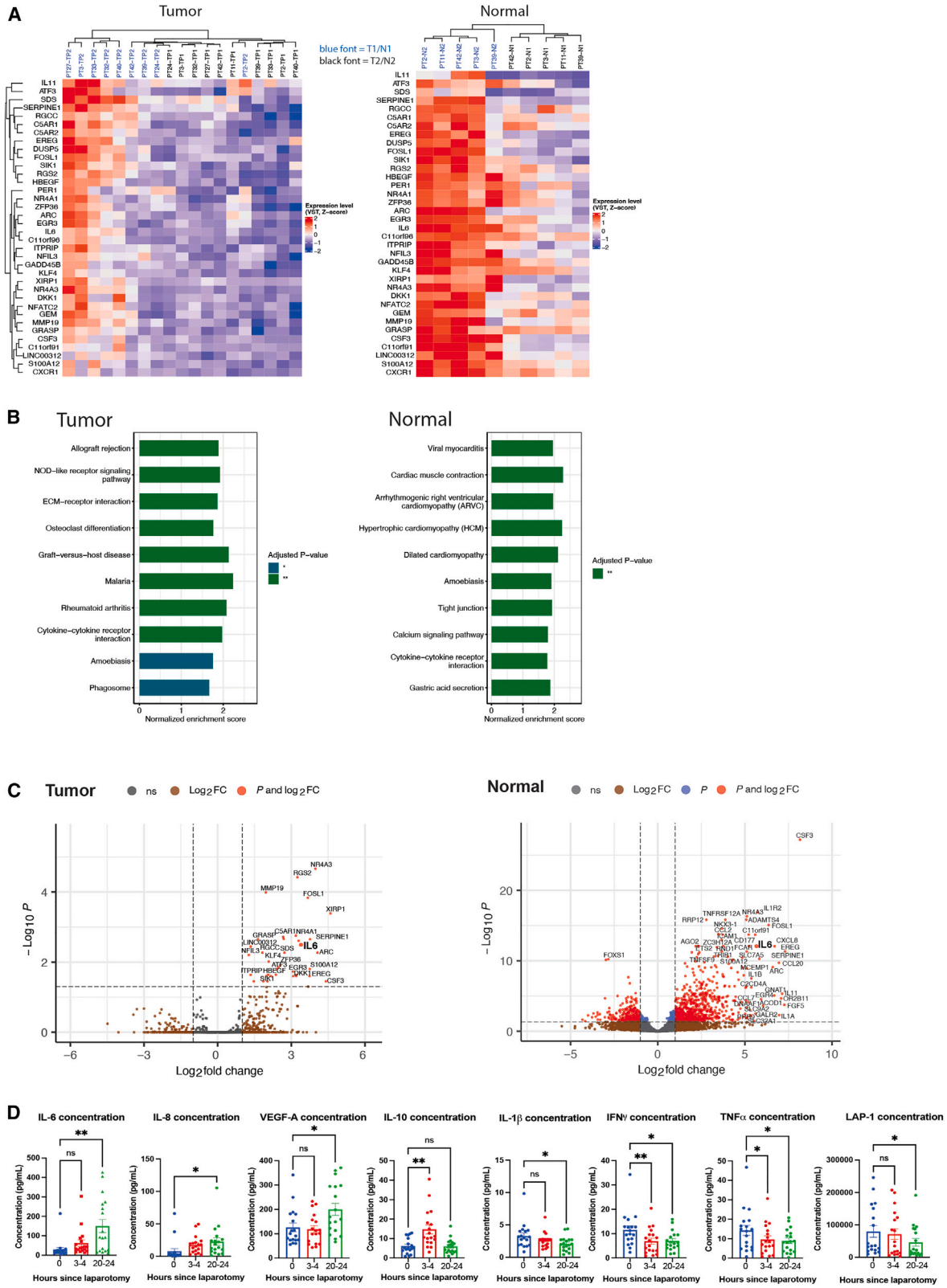

(legend on next page)

time points rather than from the same patients were clustered together (Figure 2A), implying that the observed transcriptomic changes were likely due to surgery rather than intra-patient tumor heterogeneity. All genes shown in the heatmap play a role in cellular stress response, and upregulation among these genes indicates a multi-factorial tumor cell stress response during cytoreductive surgery (Figure 2A).[18,19] Kyoto Encyclopedia of Genes and Genomes pathway analysis of differentially expressed genes in tumor and normal tissues from TP1 to TP2 revealed marked upregulation of pathways related to inflammatory response, such as those involved with cytokine–cytokine receptor interaction and a variety of infectious/autoimmune conditions (Figure 2B). We found both tumor and normal samples to be enriched for the genes related to inflammatory response, with IL-6 being one of the most upregulated genes in samples collected at TP2 compared with samples collected at TP1 ($p < 0.0001$) (Figure 2C).

To determine whether the observed changes in gene expression were potentially driven by changes in the tumor and normal tissue microenvironment, we assessed the overall levels of T cells ($CD3^+$) and myeloid/NK cells ($CD16^+$) in the TP1 and TP2 samples by IHC. We observed no significant change in percentages of $CD3^+$ or $CD16^+$ cells among tumor samples collected at the start of surgery and 3–4 h into surgery and a modest decrease in $CD16^+$ cells in normal samples collected over the same time (Figure S2).

Surgery leads to systemic inflammatory response in patients with HGSOC

Changes in transcriptional profiles in HGSOC and normal tissue samples without significant changes in the tumor microenvironment suggested that these effects were potentially driven by systemic mediators released in response to surgery. Thus, we assessed the changes in peripheral cytokine concentrations over the course of surgery and at 24 h. We observed increases in several cytokines, most notably IL-6, IL-8, and vascular endothelial growth factor A (VEGF-A), with a concomitant decrease in interferon gamma (IFNγ), IL-1β, tumor necrosis factor alpha (TNF-α), and lamina-associated polypeptide 1 (LAP-1) (Figure 2D). Notably, the changes in plasma cytokine concentrations were consistent across patients during surgery and at 20–24 h postoperatively (Figure 2D).

Surgical interventions promote tumor progression in murine cancer models and lead to immune dysfunction in the tumor microenvironment

Overall, the abovementioned findings demonstrated that surgical intervention generates a systemic inflammatory response and activation of inflammatory and potentially oncogenic signaling in tumors as early as 4 h after the initial surgical incision. Based on these observations, we hypothesized that such a systemic inflammatory response could potentially have protumorigenic effects on the minimal residual cancer remaining after surgery. To formally evaluate this in a low-tumor-burden setting, we took advantage of a newly developed syngeneic model of HGSOC driven by *myc* amplification and deletion of *TP53* and *BRCA1* (MPB),[20] and we randomized the mice bearing low peritoneal tumor burden to laparotomy vs. no intervention (Figure 3A). MPB cells were stably transduced with luciferase, which enabled *in vivo* monitoring of peritoneal tumor burden. We found that laparotomy was associated with accelerated tumor growth as assessed by bioluminescence imaging (Figures 3B, 3C, and S3). Given the accelerated tumor growth, we hypothesized that surgery has a long-term impact on the composition and/or phenotypic states of immune cells in the tumor microenvironment. Although this impact cannot be readily assessed in patients (due to tumor removal), we evaluated this in the animal MPB OC model by collecting the tumors eight days after laparotomy. Flow cytometry analysis of the mouse tumors in the laparotomy group revealed a statistically significant increase in tumor-infiltrating $CD45^+$ immune cells, including NK, CD4, and CD8 cell subsets, compared to the tumors of mice not undergoing laparotomy (Figure 3D). When focusing on the phenotypic states of the immune cells, however, we observed a decrease in NK cell activation (as evidenced by granzyme B expression) and an increase in PD-1 expression by tumor-infiltrating $CD4^+$ and $CD8^+$ T cells, consistent with increased T cell dysfunction (Figure 3D). Moreover, we noted decreased $CD8^+$ T cell activation, as evidenced by lower expression of the inducible T cell co-stimulator marker (Figure 3D).

IL-6R blockade partially restores tumor control in the setting of surgical intervention

To determine whether the increased IL-6 we observed in patients was paralleled by findings in mice, we compared IL-6 levels in mouse plasma pre-surgery and at 24 h. We observed a significant postoperative increase in median plasma IL-6 cytokine concentration (pg/μL) in mice that underwent laparotomy compared to those that did not ($p < 0.0001$) (Figure 4A). Given that IL-6 was one of the dominant genes upregulated in the human tumor samples as well as one of the dominant upregulated cytokines in both humans and mice, we next sought to determine whether IL6R blockade could potentially reverse the protumorigenic effects of surgery. We performed laparotomies on ovarian-tumor-bearing mice and treated them perioperatively with IL-6R-blocking

Figure 2. Tumor and normal tissue transcriptomic and plasma cytokine changes in patients with high-grade serous ovarian cancer undergoing cytoreductive surgery

(A) Hierarchical clustering of genes differentially expressed between high-grade serous ovarian cancer specimens from time of incision (0 h; TP1, black) and 4 h into surgery (TP2, blue). Clustered heatmap comparing upregulated genes from normal specimens from 0 h (N1, black) and 4 h (N2, blue).

(B) GSEA for tumor and normal specimens from 0 h to 4 h. $^*p < 0.05$; $^{**}p < 0.01$.

(C) Volcano plot of differentially expressed genes in high-grade serous ovarian cancer tumor specimens and normal specimens from 0 h to 4 h.

(D) Human plasma cytokine concentrations (pg/mL) from the start of surgery (blue), during surgery (3–4 h after laparotomy; red), and postoperatively (20–24 h after laparotomy; green). One-way analysis of variance with Dunnett's multiple comparisons test used for comparisons between sTP2 or sTP3 and sTP1, respectively. Data are represented as mean with standard error of mean. $^*p < 0.05$; $^{**}p < 0.01$. FC, fold change; GSEA, gene set enrichment analysis; IL, interleukin; KEGG, Kyoto Encyclopedia of Genes and Genomes; ns, not significant; VST, variance-stabilizing transformation.

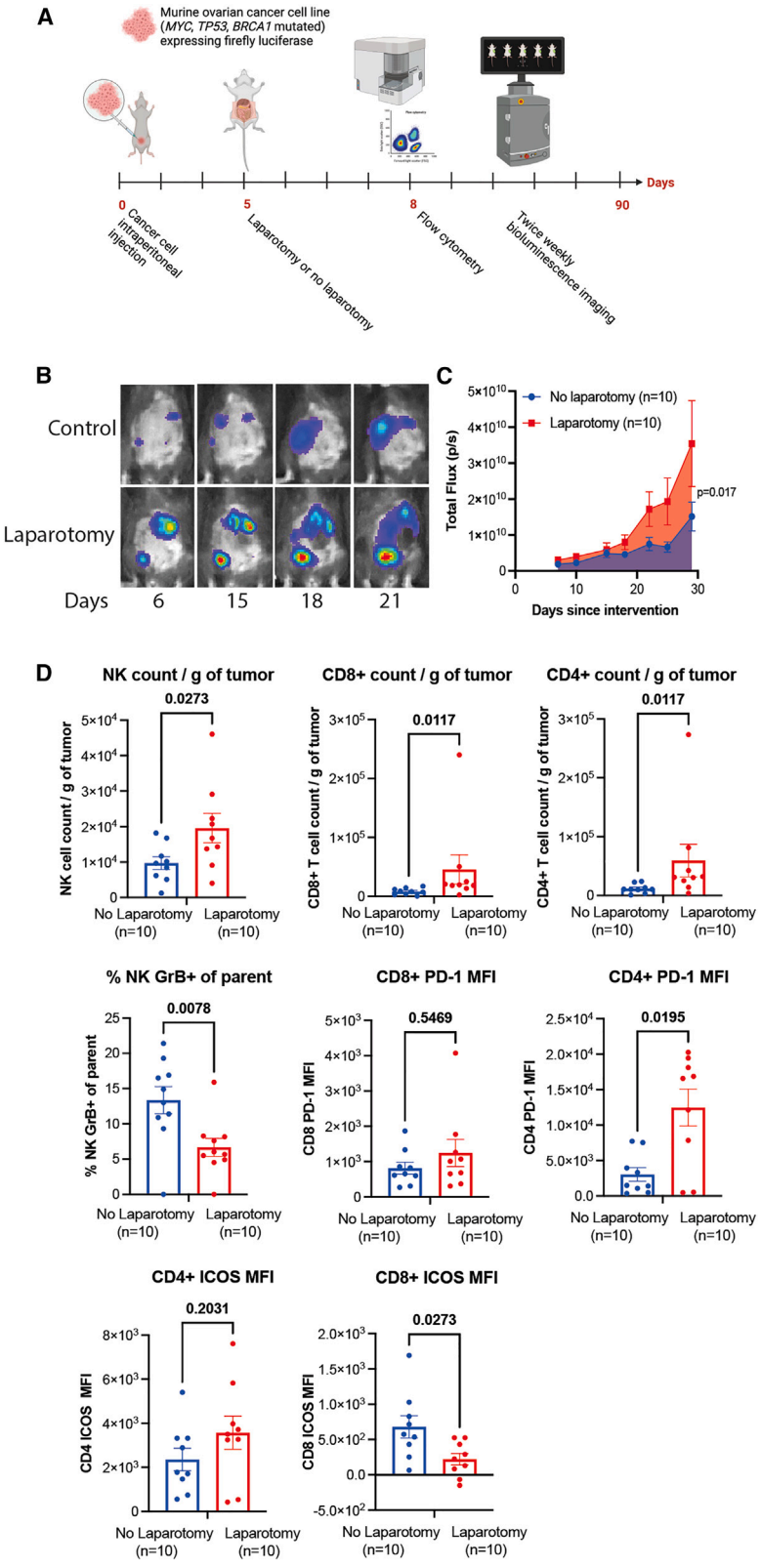

Figure 3. Surgical interventions promote tumor progression in murine cancer models and lead to immune dysfunction in the tumor microenvironment

(A) Experimental design.

(B) Representative bioluminescence imaging of a mouse inoculated with the ovarian cancer cell line and undergoing laparotomy or not, over time.

(C) Representative experiment: graphical representation of bioluminescence by luciferin uptake in ovarian cancers in mice undergoing laparotomy or not, by total flux (p/s). p = 0.017; we used Mann-Whitney U test to compare mean area under the curve between the two cohorts.

(D) Bar graph representation of various immune cell populations detected via flow cytometry of ovarian cancer tumors dissected from mice 8 days after mice either underwent laparotomy or not. We used Wilcoxon matched-pairs signed-rank test to compare percent of immune cell populations between the two groups. Data are represented as mean with standard error of mean. ICOS, inducible T cell co-stimulator; MFI, mean fluorescence intensity; NK, natural killer cell.

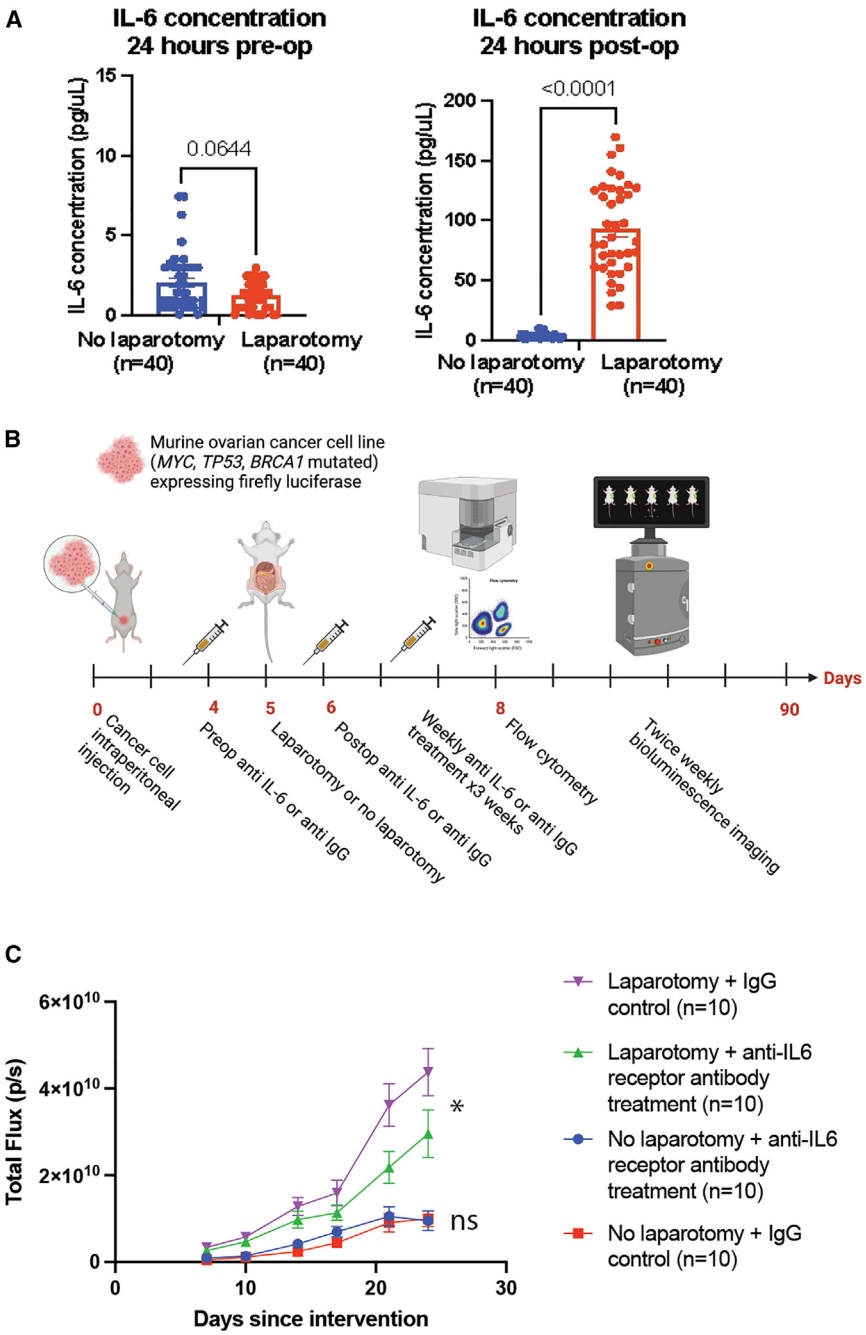

Figure 4. IL-6 receptor blockade partially restores tumor control in the setting of surgical intervention

(A) Pre- and postoperative plasma IL-6 cytokine concentration (pg/μL) for mice with ovarian cancers undergoing laparotomy or not. We used the Mann-Whitney test to compare plasma IL-6 concentration of mice undergoing laparotomy or not.

(B) Experimental design.

(C) Representative experiment: graphical representation of bioluminescence by luciferin uptake in ovarian cancer tumors in mice undergoing laparotomy treated with either control IgG or anti-IL6R antibody, by total flux (p/s). We also compared bioluminescence by luciferin uptake in ovarian cancer tumors in mice not undergoing laparotomy treated with either control IgG or anti-IL6R antibody, by total flux (p/s). We used Mann-Whitney U test to compare mean area under the curve between the two groups. Data are represented as mean with standard error of mean. *$p < 0.05$. IL, interleukin; IL-6R, interleukin-6 receptor; ns, not significant.

antibody or control immunoglobulin G (IgG) (Figure 4B). Although IL-6R blockade had no effect on growth of tumors in mice that did not undergo laparotomy, blockade of IL-6R resulted in partial restoration of tumor control in animals who underwent laparotomy (Figures 4C and S4).

DISCUSSION

Multi-site analyses of HGSOC performed by our group have previously demonstrated substantial inter-site heterogeneity in immune infiltration and cancer-cell-intrinsic signaling.[21] Our current data provide insight into the temporal comparison of tumor specimens collected at the start of surgery and 3–4 h into surgery and demonstrate that beyond the spatial heterogeneity, timing of specimen collection can reflect the apparent transcriptional signatures identified in OCs. Thus, we posit that timing of specimen collection in relation to surgical incision should be considered a factor when interpreting transcriptional data from OCs. Importantly, the multi-time collection of biospecimens in our study enabled evaluation of the evolution of intratumoral and peripheral changes as a response to laparotomy/PCS.

Our results add to the growing body of literature demonstrating the impact of surgical stress on the tumor microenvironment with potential to promote tumorigenesis.[7,8,11,22,23] The dilemma of performing necessary cytoreductive surgery for tumor debulking with the possible pro-tumorigenic systemic effects of multi-hour, stress-inducing surgery has been previously described in various solid tumors.[8,11,16,17,23] In HGSOCs and normal tissue specimens collected throughout PCS, we show that surgery leads to induction of inflammatory stress signatures at the transcriptional level and in peripheral blood, with IL-6 emerging as a dominant inflammatory pathway. Although our study had too few cases to perform meaningful outcomes assessments, prior work has demonstrated the prognostic value of plasma IL-6 concentration in patients with ovarian cancer.[14,16] Additional studies in the

neoadjuvant chemotherapy setting have also demonstrated a correlation between tumor upregulation of IL-6 and chemotherapy or platinum resistance.[24,25] Although it is not known if upregulation of intratumoral and peripheral IL-6 during cytoreductive surgery contributes to subsequent chemotherapy resistance, additional evaluation of anti-cytokine therapeutics during or in the immediate perioperative time and its impact on subsequent chemo-resistance is warranted.[17,26–28]

In our study, we observed only a modest reduction in tumorigenesis after perioperative treatment with anti-IL-6R antibody in the murine model. The lack of complete tumor growth inhibition could be attributed to several factors, including the importance of IL-6 in MPB model tumorigenesis and potentially other factors contributing to tumorigenesis aside from increased peripheral and intratumoral IL-6.[6,9,10,22,29–32] Other murine model studies have demonstrated the benefit of IL-6 blockade in tumorigenesis.[22] In a syngeneic murine model of acute lymphoblastic leukemia, Bent et al. have demonstrated that IL-6 knockout mice treated with doxorubicin completely clear leukemic cells, with most mice undergoing T-cell-dependent anti-leukemia immune responses.[13] In xenograft models including an OC cell line, Zhong et al. have demonstrated that MEDI5117 (a human monoclonal antibody that potently binds and neutralizes human IL-6) inhibits tumor growth.[32] At the transcriptomic level, they also demonstrated downregulation of SOCS3 (suppression of cytokine signaling 3) mRNA by MEDI5117, which is typically induced by IL-6, IL-10, and IFNγ cytokines.[32] Kim et al. similarly reported that selective knockdown of IL-6R or inhibition with IL-6-neutralizing antibody suppressed the stimulatory effects of ascites on OC invasion.[9] These studies, in line with our results, generate a rationale for further studies of anti-IL-6 treatment in reducing surgical-stress-induced tumorigenesis in the perioperative period.

In addition to an increase in plasma IL-6 levels, we have also observed an increase in IL-8 and VEGF-A throughout PCS and 20–24 h after PCS, highlighting that blockade of additional pathways may be necessary to reverse perioperative stress-related tumorigenesis.[33,34] In an *in vitro* human OC model, Zhang et al. demonstrated the effectiveness of co-targeting the IL-6 and IL-8 pathways with bazedoxifene and SCH527123 treatment.[35] Auer et al. have also shown the ability to reverse postoperative NK cell dysfunction with anti-transforming growth factor β (TGF-β) immunotherapeutics in patients undergoing surgery for colorectal cancer.[36–38] Lastly, Dijkgraaf et al. reported on the feasibility, safety, and evidence of immune activation with administration of tocilizumab (IL-6R blockade) alongside carboplatin and pegylated liposomal doxorubicin in patients with recurrent OC.[39] Alongside other cytokine changes, our study demonstrates increased PD-1 expression in tumor-infiltrating T cells, suggesting a potential increase in T cell dysfunction in the tumor microenvironment after laparotomy (Figure 3D). Although PD-1/PD-L1 inhibitors alone have not shown tremendous benefit in ovarian cancer treatment, our results nevertheless generate rationale for perioperative PD-1/PD-L1 blockade in combination with other strategies.

Aside from anti-cytokine mechanisms to reduce postoperative tumorigenesis, studies in various animal models and human early phase clinical trials have investigated other anti-stress or anti-cancer therapeutics in the perioperative period.[11,23,40] Auer et al. have demonstrated that low-molecular-weight heparins can effectively reduce metastatic burden and decrease tumor growth in preclinical animal models of solid tumor malignancies.[41] In a clinical trial, however, there was no improvement in disease-free or overall survival in patients with colorectal cancer undergoing surgical resection receiving extended perioperative anticoagulation with tinzaparin vs. in-patient prophylaxis alone.[42,43] Perioperative beta-blockade has also been investigated as an anti-stress mechanism in patients with breast and colorectal cancers, with favorable changes in prometastatic and proinflammatory transcription factors in excised breast cancer and colorectal cancer tissue and a notable improvement in disease-free survival in patients with colorectal cancer.[26,27,44] A randomized controlled feasibility trial for patients with advanced-stage HGSOC is now open at MSK (the PRESERVE trial; NCT05429970) that utilizes various anti-stress methods. Further clinical trials are warranted for patients with OC to help clinicians understand the safety and possible benefits of perioperative stress pathway blockade.

In summary, our findings indicate that laparotomy induces an intratumoral and peripheral inflammatory response in patients with HGSOC and accelerates tumor growth in mice. Our study provides important insights into the stress pathways activated by surgery and generates rationale for perioperative therapeutic interventions to reduce the protumorigenic effects of surgery and thereby optimize the outcomes of cytoreductive surgery.

Limitations of the study

Our study is limited by the small sample size of the overall number of human subjects included. Thus, these results are exploratory and hypothesis generating. However, despite the small sample size, we observed a consistent signal among the murine and human results, indicating the tumorigenic effect of laparotomy and potential for perioperative therapeutic blockade to reduce these effects. Further investigation of perioperative stress blockade in humans is needed to understand the effect on laparotomy-induced tumorigenesis. Moreover, our work only assessed tumors of patients undergoing primary cytoreductive surgery to study a homogeneous group of chemo-naïve tumors, and comparison to tumors exposed to neoadjuvant chemotherapy and then interval cytoreductive surgery would be of clinical interest. Lastly, although our study only focused on the immune factors, there are additional biological systems at play in the tumorigenic sequelae after laparotomy that warrant further evaluation.

RESOURCE AVAILABILITY

Lead contact

Requests for further information and resources should be directed to and will be fulfilled by the lead contact, Dmitriy Zamarin (Dmitriy.Zamarin@mssm.edu).

Materials availability

This study did not generate new unique reagents.

Data and code availability

- RNAseq data have been deposited at Synapse and are currently available:
  - Tumor RNAseq data: https://doi.org/10.7303/syn64364142
  - Normal RNAseq data: https://doi.org/10.7303/syn64364380

- This paper does not report original code.
- Any additional information required to reanalyze the data reported in this paper is available from the lead contact upon request.

ACKNOWLEDGMENTS

D.Z. is funded in part by the National Institutes of Health/National Cancer Institute Cancer Center Support Grant (P30-CA196521-09), Ovarian Cancer Research Alliance Liz Tilberis Award, and National Cancer Institute R01 (R01CA269382). This research was funded in part by the NIH/NCI Cancer Center Support Grant P30 CA008748 to Memorial Sloan Kettering Cancer Center. B.W. is supported in part by Cycle for Survival, NIH/NCI (P50 CA247749), and Breast Cancer Research Foundation grants. The authors used Biorender.com to create Figures 1A, 3A, and 4B.

AUTHOR CONTRIBUTIONS

A.M.P., conceptualization, experimental design, data curation, methodology, original draft writing, review and editing. L.A.M., experimental design, data curation, methodology, review and editing. Y.Z., data curation, bioinformatics, formal analysis, review and editing. A.L.F.L., experimental design, formal analysis, methodology, review and editing. F.D., pathology review, formal analysis, data curation, review and editing. T.H., methodology, review and editing. G.P., methodology, review and editing. H.G., methodology, review and editing. M.A.O., methodology, review and editing. E.H., methodology, review and editing. R.K., methodology, review and editing. M.B., methodology, review and editing. T.S., methodology, review and editing. N.R.A.-R., review and editing. G.G., review and editing. K.L.R., review and editing. Y.S., review and editing. O.Z., review and editing. D.S.C., review and editing. T.M., experimental design, methodology, review and editing. R.G., methodology, review and editing. B.W., experimental design, methodology, review and editing. D.Z., conceptualization, experimental design, data curation, formal analysis, methodology, original draft writing, review and editing, supervision.

DECLARATION OF INTERESTS

N.R.A.-R. reports grants from GRAIL paid to his institution. D.S.C. reports speaker honoraria from AstraZeneca; advisory board participation for Verthermia Acquio and Biom 'Up; and stock or stock options in Doximity and BioNTech SE. T.M. reports consultant work for Immunos Therapeutics, Daiichi Sankyo Co, TigaTx, Normunity and Pfizer; being a cofounder of and holding equity in: IMVAQ Therapeutics; reports previous research funding from Surface Oncology, Kyn Therapeutics, Infinity Pharmaceuticals, Peregrine Pharmaceuticals, Adaptive Biotechnologies, Leap Therapeutics, and Aprea Therapeutics; reports current research funding from Bristol-Myers Squibb, Enterome SA, and Realta Life Sciences; and reports patent applications related to work on oncolytic viral therapy, alpha virus–based vaccine, *neo*antigen modeling, CD40, GITR, OX40, PD-1, and CTLA-4. B.W. reports grants from Repare Therapeutics and SAGA Diagnostics paid to her institution and employment of a direct family member at AstraZeneca. D.Z. reports institutional grants from Merck, Genentech, AstraZeneca, and Synthekine; personal fees from AstraZeneca, Xencor, Memgen, Daichi Sankyo, Gilead, Synthekine, Immunos, Hervolution, Accurius, and Calidi Biotherapeutics; and patent ownership on use of oncolytic Newcastle Disease Virus for cancer therapy. A.M.P., L.A.M., Y.Z., A.L.F.L., F.D., T.H., G.P., H.G., M.A.O., E.H., R.K., M.N.B., T.S., G.G., K.L.R., Y.S., O.Z., and R.G. report no conflicts.

STAR★METHODS

Detailed methods are provided in the online version of this paper and include the following:

SUPPLEMENTAL INFORMATION

Supplemental information can be found online at https://doi.org/10.1016/j.isci.2025.112317.

Received: December 11, 2024
Revised: January 28, 2025
Accepted: March 25, 2025
Published: March 28, 2025

REFERENCES

1. Siegel, R.L., Giaquinto, A.N., and Jemal, A. (2024). Cancer statistics, 2024. CA Cancer J. Clin. *74*, 12–49. https://doi.org/10.3322/caac.21820.
2. Tai, L.H., and Auer, R. (2014). Attacking Postoperative Metastases using Perioperative Oncolytic Viruses and Viral Vaccines. Front. Oncol. *4*, 217. https://doi.org/10.3389/fonc.2014.00217.
3. Tai, L.H., de Souza, C.T., Bélanger, S., Ly, L., Alkayyal, A.A., Zhang, J., Rintoul, J.L., Ananth, A.A., Lam, T., Breitbach, C.J., et al. (2013). Preventing postoperative metastatic disease by inhibiting surgery-induced dysfunction in natural killer cells. Cancer Res. *73*, 97–107. https://doi.org/10.1158/0008-5472.CAN-12-1993.
4. Tai, L.H., Tanese de Souza, C., Sahi, S., Zhang, J., Alkayyal, A.A., Ananth, A.A., and Auer, R.A.C. (2014). A mouse tumor model of surgical stress to explore the mechanisms of postoperative immunosuppression and evaluate novel perioperative immunotherapies. J. Vis. Exp. *85*, 51253. https://doi.org/10.3791/51253.
5. Seth, R., Tai, L.H., Falls, T., de Souza, C.T., Bell, J.C., Carrier, M., Atkins, H., Boushey, R., and Auer, R.A. (2013). Surgical stress promotes the development of cancer metastases by a coagulation-dependent mechanism involving natural killer cells in a murine model. Ann. Surg. *258*, 158–168. https://doi.org/10.1097/SLA.0b013e31826fcbdb.
6. Browning, L., Patel, M.R., Horvath, E.B., Tawara, K., and Jorcyk, C.L. (2018). IL-6 and ovarian cancer: inflammatory cytokines in promotion of metastasis. Cancer Manag. Res. *10*, 6685–6693. https://doi.org/10.2147/CMAR.S179189.
7. Coffey, J.C., Wang, J.H., Smith, M.J.F., Bouchier-Hayes, D., Cotter, T.G., and Redmond, H.P. (2003). Excisional surgery for cancer cure: therapy at a cost. Lancet Oncol. *4*, 760–768. https://doi.org/10.1016/s1470-2045(03)01282-8.
8. Lange, P.H., Hekmat, K., Bosl, G., Kennedy, B.J., and Fraley, E.E. (1980). Acclerated growth of testicular cancer after cytoreductive surgery. Cancer *45*, 1498–1506. https://doi.org/10.1002/1097-0142(19800315)45:6<1498::aid-cncr2820450633>3.0.co;2-7.
9. Kim, S., Gwak, H., Kim, H.S., Kim, B., Dhanasekaran, D.N., and Song, Y.S. (2016). Malignant ascites enhances migratory and invasive properties of ovarian cancer cells with membrane bound IL-6R in vitro. Oncotarget *7*, 83148–83159. https://doi.org/10.18632/oncotarget.13074.
10. Wang, Y., Li, L., Guo, X., Jin, X., Sun, W., Zhang, X., and Xu, R.C. (2012). Interleukin-6 signaling regulates anchorage-independent growth, proliferation, adhesion and invasion in human ovarian cancer cells. Cytokine *59*, 228–236. https://doi.org/10.1016/j.cyto.2012.04.020.

11. Matzner, P., Sandbank, E., Neeman, E., Zmora, O., Gottumukkala, V., and Ben-Eliyahu, S. (2020). Harnessing cancer immunotherapy during the unexploited immediate perioperative period. Nat. Rev. Clin. Oncol. *17*, 313–326. https://doi.org/10.1038/s41571-019-0319-9.

12. Szulc-Kielbik, I., Kielbik, M., Nowak, M., and Klink, M. (2021). The implication of IL-6 in the invasiveness and chemoresistance of ovarian cancer cells. Systematic review of its potential role as a biomarker in ovarian cancer patients. Biochim. Biophys. Acta. Rev. Cancer *1876*, 188639. https://doi.org/10.1016/j.bbcan.2021.188639.

13. Maccio, A., and Madeddu, C. (2012). Inflammation and ovarian cancer. Cytokine *58*, 133–147. https://doi.org/10.1016/j.cyto.2012.01.015.

14. Alvarez Secord, A., Bell Burdett, K., Owzar, K., Tritchler, D., Sibley, A.B., Liu, Y., Starr, M.D., Brady, J.C., Lankes, H.A., Hurwitz, H.I., et al. (2020). Predictive Blood-Based Biomarkers in Patients with Epithelial Ovarian Cancer Treated with Carboplatin and Paclitaxel with or without Bevacizumab: Results from GOG-0218. Clin. Cancer Res. *26*, 1288–1296. https://doi.org/10.1158/1078-0432.CCR-19-0226.

15. Burger, R.A., Brady, M.F., Bookman, M.A., Fleming, G.F., Monk, B.J., Huang, H., Mannel, R.S., Homesley, H.D., Fowler, J., Greer, B.E., et al. (2011). Incorporation of bevacizumab in the primary treatment of ovarian cancer. N. Engl. J. Med. *365*, 2473–2483. https://doi.org/10.1056/NEJMoa1104390.

16. Stone, R.L., Nick, A.M., McNeish, I.A., Balkwill, F., Han, H.D., Bottsford-Miller, J., Rupairmoole, R., Armaiz-Pena, G.N., Pecot, C.V., Coward, J., et al. (2012). Paraneoplastic thrombocytosis in ovarian cancer. N. Engl. J. Med. *366*, 610–618. https://doi.org/10.1056/NEJMoa1110352.

17. Tseng, J.H., Cowan, R.A., Afonso, A.M., Zhou, Q., Iasonos, A., Ali, N., Thompson, E., Sonoda, Y., O'Cearbhaill, R.E., Chi, D.S., et al. (2018). Perioperative epidural use and survival outcomes in patients undergoing primary debulking surgery for advanced ovarian cancer. Gynecol. Oncol. *151*, 287–293. https://doi.org/10.1016/j.ygyno.2018.08.024.

18. Muralidharan, S., and Mandrekar, P. (2013). Cellular stress response and innate immune signaling: integrating pathways in host defense and inflammation. J. Leukoc. Biol. *94*, 1167–1184. https://doi.org/10.1189/jlb.0313153.

19. Hai, T., Wolfgang, C.D., Marsee, D.K., Allen, A.E., and Sivaprasad, U. (1999). ATF3 and stress responses. Gene Expr. *7*, 321–335.

20. Paffenholz, S.V., Salvagno, C., Ho, Y.J., Limjoco, M., Baslan, T., Tian, S., Kulick, A., de Stanchina, E., Wilkinson, J.E., Barriga, F.M., et al. (2022). Senescence induction dictates response to chemo- and immunotherapy in preclinical models of ovarian cancer. Proc. Natl. Acad. Sci. USA *119*, e2117754119. https://doi.org/10.1073/pnas.2117754119.

21. Vazquez-Garcia, I., Uhlitz, F., Ceglia, N., Lim, J.L.P., Wu, M., Mohibullah, N., Niyazov, J., Ruiz, A.E.B., Boehm, K.M., Bojilova, V., et al. (2022). Ovarian cancer mutational processes drive site-specific immune evasion. Nature *612*, 778–786. https://doi.org/10.1038/s41586-022-05496-1.

22. Bent, E.H., Millán-Barea, L.R., Zhuang, I., Goulet, D.R., Fröse, J., and Hemann, M.T. (2021). Microenvironmental IL-6 inhibits anti-cancer immune responses generated by cytotoxic chemotherapy. Nat. Commun. *12*, 6218. https://doi.org/10.1038/s41467-021-26407-4.

23. Goldfarb, Y., Sorski, L., Benish, M., Levi, B., Melamed, R., and Ben-Eliyahu, S. (2011). Improving postoperative immune status and resistance to cancer metastasis: a combined perioperative approach of immunostimulation and prevention of excessive surgical stress responses. Ann. Surg. *253*, 798–810. https://doi.org/10.1097/SLA.0b013e318211d7b5.

24. Arend, R.C., Londoño, A.I., Montgomery, A.M., Smith, H.J., Dobbin, Z.C., Katre, A.A., Martinez, A., Yang, E.S., Alvarez, R.D., Huh, W.K., et al. (2018). Molecular Response to Neoadjuvant Chemotherapy in High-Grade Serous Ovarian Carcinoma. Mol. Cancer Res. *16*, 813–824. https://doi.org/10.1158/1541-7786.MCR-17-0594.

25. Javellana, M., Eckert, M.A., Heide, J., Zawieracz, K., Weigert, M., Ashley, S., Stock, E., Chapel, D., Huang, L., Yamada, S.D., et al. (2022). Neoadjuvant Chemotherapy Induces Genomic and Transcriptomic Changes in Ovarian Cancer. Cancer Res. *82*, 169–176. https://doi.org/10.1158/0008-5472.CAN-21-1467.

26. Musselman, R.P., Bennett, S., Li, W., Mamdani, M., Gomes, T., van Walraven, C., Boushey, R., Al-Obeed, O., Al-Omran, M., and Auer, R.C. (2018). Association between perioperative beta blocker use and cancer survival following surgical resection. Eur. J. Surg. Oncol. *44*, 1164–1169. https://doi.org/10.1016/j.ejso.2018.05.012.

27. Ricon-Becker, I., Haldar, R., Shabat Simon, M., Gutman, M., Cole, S.W., Ben-Eliyahu, S., and Zmora, O. (2023). Effect of perioperative COX-2 and beta-adrenergic inhibition on 5-year disease-free-survival in colorectal cancer: A pilot randomized controlled Colorectal Metastasis PreventIon Trial (COMPIT). Eur. J. Surg. Oncol. *49*, 655–661. https://doi.org/10.1016/j.ejso.2022.10.013.

28. Shaashua, L., Shabat-Simon, M., Haldar, R., Matzner, P., Zmora, O., Shabtai, M., Sharon, E., Allweis, T., Barshack, I., Hayman, L., et al. (2017). Perioperative COX-2 and beta-Adrenergic Blockade Improves Metastatic Biomarkers in Breast Cancer Patients in a Phase-II Randomized Trial. Clin. Cancer Res. *23*, 4651–4661. https://doi.org/10.1158/1078-0432.CCR-17-0152.

29. Aaboud, M., Aad, G., Abbott, B., Abdinov, O., Abeloos, B., Abhayasinghe, D., Abidi, S., AbouZeid, O., Abraham, N., Abramowicz, H., et al. (2019). Comparison of Fragmentation Functions for Jets Dominated by Light Quarks and Gluons from pp and Pb+Pb Collisions in ATLAS. Phys. Rev. Lett. *123*, 042001. https://doi.org/10.1103/PhysRevLett.123.042001.

30. Raskova, M., Lacina, L., Kejik, Z., Venhauerová, A., Skaličková, M., Kolář, M., Jakubek, M., Rosel, D., Smetana, K., Jr., and Brábek, J. (2022). The Role of IL-6 in Cancer Cell Invasiveness and Metastasis-Overview and Therapeutic Opportunities. Cells *11*, 3698. https://doi.org/10.3390/cells11223698.

31. Rossi, J.F., Lu, Z.Y., Jourdan, M., and Klein, B. (2015). Interleukin-6 as a therapeutic target. Clin. Cancer Res. *21*, 1248–1257. https://doi.org/10.1158/1078-0432.CCR-14-2291.

32. Zhong, H., Davis, A., Ouzounova, M., Carrasco, R.A., Chen, C., Breen, S., Chang, Y.S., Huang, J., Liu, Z., Yao, Y., et al. (2016). A Novel IL6 Antibody Sensitizes Multiple Tumor Types to Chemotherapy Including Trastuzumab-Resistant Tumors. Cancer Res. *76*, 480–490. https://doi.org/10.1158/0008-5472.CAN-15-0883.

33. Fousek, K., Horn, L.A., and Palena, C. (2021). Interleukin-8: A chemokine at the intersection of cancer plasticity, angiogenesis, and immune suppression. Pharmacol. Ther. *219*, 107692. https://doi.org/10.1016/j.pharmthera.2020.107692.

34. Hicklin, D.J., and Ellis, L.M. (2005). Role of the vascular endothelial growth factor pathway in tumor growth and angiogenesis. J. Clin. Oncol. *23*, 1011–1027. https://doi.org/10.1200/JCO.2005.06.081.

35. Zhang, R., Roque, D.M., Reader, J., and Lin, J. (2022). Combined inhibition of IL-6 and IL-8 pathways suppresses ovarian cancer cell viability and migration and tumor growth. Int. J. Oncol. *60*, 50. https://doi.org/10.3892/ijo.2022.5340.

36. Market, M., Tennakoon, G., and Auer, R.C. (2021). Postoperative Natural Killer Cell Dysfunction: The Prime Suspect in the Case of Metastasis Following Curative Cancer Surgery. Int. J. Mol. Sci. *22*, 11378. https://doi.org/10.3390/ijms222111378.

37. Angka, L., Khan, S.T., Kilgour, M.K., Xu, R., Kennedy, M.A., and Auer, R.C. (2017). Dysfunctional Natural Killer Cells in the Aftermath of Cancer Surgery. Int. J. Mol. Sci. *18*, 1787. https://doi.org/10.3390/ijms18081787.

38. Market, M., Tennakoon, G., Scaffidi, M., Cook, D.P., Angka, L., Ng, J., Tanese de Souza, C., Kennedy, M.A., Vanderhyden, B.C., and Auer, R.C. (2022). Preventing Surgery-Induced NK Cell Dysfunction Using Anti-TGF-beta Immunotherapeutics. Int. J. Mol. Sci. *23*, 14608. https://doi.org/10.3390/ijms232314608.

39. Dijkgraaf, E.M., Santegoets, S.J.A.M., Reyners, A.K.L., Goedemans, R., Wouters, M.C.A., Kenter, G.G., van Erkel, A.R., van Poelgeest, M.I.E., Nijman, H.W., van der Hoeven, J.J.M., et al. (2015). A phase I trial combining carboplatin/doxorubicin with tocilizumab, an anti-IL-6R monoclonal

antibody, and interferon-alpha2b in patients with recurrent epithelial ovarian cancer. Ann. Oncol. *26*, 2141–2149. https://doi.org/10.1093/annonc/mdv309.

40. Levi, B., Matzner, P., Goldfarb, Y., Sorski, L., Shaashua, L., Melamed, R., Rosenne, E., Page, G.G., and Ben-Eliyahu, S. (2016). Stress impairs the efficacy of immune stimulation by CpG-C: Potential neuroendocrine mediating mechanisms and significance to tumor metastasis and the perioperative period. Brain Behav. Immun. *56*, 209–220. https://doi.org/10.1016/j.bbi.2016.02.025.
41. Ripsman, D., Fergusson, D.A., Montroy, J., Auer, R.C., Huang, J.W., Dobriyal, A., Wesch, N., Carrier, M., and Lalu, M.M. (2020). A systematic review on the efficacy and safety of low molecular weight heparin as an anticancer therapeutic in preclinical animal models. Thromb. Res. *195*, 103–113. https://doi.org/10.1016/j.thromres.2020.07.008.
42. Auer, R., Scheer, A., Wells, P.S., Boushey, R., Asmis, T., Jonker, D., and Carrier, M. (2011). The use of extended perioperative low molecular weight heparin (tinzaparin) to improve disease-free survival following surgical resection of colon cancer: a pilot randomized controlled trial. Blood Coagul. Fibrinolysis *22*, 760–762. https://doi.org/10.1097/MBC.0b013e328349f1a8.
43. Auer, R.C., Ott, M., Karanicolas, P., Brackstone, M.R., Ashamalla, S., Weaver, J., Tagalakis, V., Boutros, M., Stotland, P., Marulanda, A.C., et al. (2022). Efficacy and safety of extended duration to perioperative thromboprophylaxis with low molecular weight heparin on disease-free survival after surgical resection of colorectal cancer (PERIOP-01): multicentre, open label, randomised controlled trial. BMJ *378*, e071375. https://doi.org/10.1136/bmj-2022-071375.
44. Ricon, I., Hanalis-Miller, T., Haldar, R., Jacoby, R., and Ben-Eliyahu, S. (2019). Perioperative biobehavioral interventions to prevent cancer recurrence through combined inhibition of beta-adrenergic and cyclooxygenase 2 signaling. Cancer *125*, 45–56. https://doi.org/10.1002/cncr.31594.
45. Kim, S.H., Da Cruz Paula, A., Basili, T., Dopeso, H., Bi, R., Pareja, F., da Silva, E.M., Gularte-Mérida, R., Sun, Z., Fujisawa, S., et al. (2020). Identification of recurrent FHL2-GLI2 oncogenic fusion in sclerosing stromal tumors of the ovary. Nat. Commun. *11*, 44. https://doi.org/10.1038/s41467-019-13806-x.
46. Basili, T., Dopeso, H., Kim, S.H., Ferrando, L., Pareja, F., Da Cruz Paula, A., da Silva, E.M., Stylianou, A., Maroldi, A., Marchiò, C., et al. (2020). Oncogenic properties and signaling basis of the PAX8-GLIS3 fusion gene. Int. J. Cancer *147*, 2253–2264. https://doi.org/10.1002/ijc.33040.
47. Dobin, A., Davis, C.A., Schlesinger, F., Drenkow, J., Zaleski, C., Jha, S., Batut, P., Chaisson, M., and Gingeras, T.R. (2013). STAR: ultrafast universal RNA-seq aligner. Bioinformatics *29*, 15–21. https://doi.org/10.1093/bioinformatics/bts635.
48. Lawrence, M., Huber, W., Pagès, H., Aboyoun, P., Carlson, M., Gentleman, R., Morgan, M.T., and Carey, V.J. (2013). Software for computing and annotating genomic ranges. PLoS Comput. Biol. *9*, e1003118. https://doi.org/10.1371/journal.pcbi.1003118.
49. Gentleman, R.C., Carey, V.J., Bates, D.M., Bolstad, B., Dettling, M., Dudoit, S., Ellis, B., Gautier, L., Ge, Y., Gentry, J., et al. (2004). Bioconductor: open software development for computational biology and bioinformatics. Genome Biol. *5*, R80. https://doi.org/10.1186/gb-2004-5-10-r80.
50. Love, M.I., Huber, W., and Anders, S. (2014). Moderated estimation of fold change and dispersion for RNA-seq data with DESeq2. Genome Biol. *15*, 550. https://doi.org/10.1186/s13059-014-0550-8.
51. Yu, G., Wang, L.G., Han, Y., and He, Q.Y. (2012). clusterProfiler: an R package for comparing biological themes among gene clusters. OMICS *16*, 284–287. https://doi.org/10.1089/omi.2011.0118.
52. Wang, G., Xu, D., Zhang, Z., Li, X., Shi, J., Sun, J., Liu, H.Z., Li, X., Zhou, M., and Zheng, T. (2021). The pan-cancer landscape of crosstalk between epithelial-mesenchymal transition and immune evasion relevant to prognosis and immunotherapy response. npj Precis. Oncol. *5*, 56. https://doi.org/10.1038/s41698-021-00200-4.
53. Cunha, L.L., Nonogaki, S., Soares, F.A., Vassallo, J., and Ward, L.S. (2017). Immune Escape Mechanism is Impaired in the Microenvironment of Thyroid Lymph Node Metastasis. Endocr. Pathol. *28*, 369–372. https://doi.org/10.1007/s12022-017-9495-2.
54. Hu, J.Q., Lei, B.W., Wen, D., Ma, B., Zhang, T.T., Lu, Z.W., Wei, W.J., Wang, Y.L., Wang, Y., Li, D.S., et al. (2020). IL-2 enhanced MHC class I expression in papillary thyroid cancer with Hashimoto's thyroiditis overcomes immune escape in vitro. J. Cancer *11*, 4250–4260. https://doi.org/10.7150/jca.38330.
55. van Diest, P.J., van Dam, P., Henzen-Logmans, S.C., Berns, E., van der Burg, M.E., Green, J., and Vergote, I. (1997). A scoring system for immunohistochemical staining: consensus report of the task force for basic research of the EORTC-GCCG. European Organization for Research and Treatment of Cancer-Gynaecological Cancer Cooperative Group. J Clin Pathol. *50*, 801–804. https://doi.org/10.1136/jcp.50.10.801.

STAR★METHODS

KEY RESOURCES TABLE

REAGENT or RESOURCE	SOURCE	IDENTIFIER
Antibodies		
*InVivo*MAb anti-mouse IL-6R	BioxCell	Cat#BE0047; RRID: AB_1107588
*InVivo*MAb rat IgG2b isotype control, anti-keyhole limpet hemocyanin	BioxCell	Cat#BE0090; RRID: AB_1107780
Zombie-NIR dye	BioLegend	Cat#423106; RRID: unknown
CD45-BUV563	BD Biosciences	Cat#565710; RRID: AB2722550
CD3-APC/Fire810	BioLegend	Cat#100267; RRID: AB_2876392
CD4-BUV805	BD Biosciences	Cat#612900; RRID: AB_2827960
CD8a-BUV615	BD Biosciences	Cat#613004; RRID: AB_2870272
NK1.1-BUV661	BD Biosciences	Cat#741477; RRID: AB_2870942
CD11b-BV510	BioLegend	Cat#101245; RRID: AB_2561390
I-A/I-E-SparkBlue550	BioLegend	Cat#107661; RRID: AB_2876418
CD86-SB702	Invitrogen	Cat#67-086-282; RRID: AB_2717155
PDL1-BV480	BD Biosciences	Cat#568589; RRID: unknown
ICOS-PE	Invitrogen	Cat#12-9942-82; RRID: AB_466274
PD-1-BV785	BioLegend	Cat#135225; RRID: AB_2563680
FoxP3-PerCP-eF710	Invitrogen	Cat#46-5773-82; RRID: AB_914351
Granzyme B-APC	Invitrogen	Cat#GRB05; RRID: AB_2536539
CD16 [Clone 2H7]	Leica	Cat# CD16-L-U; RRID: unknown
CD3 [Clone LN10]	Leica	Cat# PA0553-U; RRID: unknown
Biological samples		
Human: high-grade serous ovarian cancer tissue samples	This paper	
Human: high-grade serous ovarian cancer blood samples	This paper	
Mouse: cell cultures	This paper	
Mouse: blood samples	This paper	
Chemicals, peptides, and recombinant proteins		
1% penicillin/streptomycin	Gibco	Cat# 15-070-063
10% fetal bovine serum	Gemini Biosciences	Cat# S11150
RPMI 1640 medium	Corning	Cat# 10-041-CV
Percoll 40%	Sigma-Aldrich	Cat# P1644
Liberase TL	Roche	Cat# 05401020001
DNAase 1	Roche	Cat# 10104159001
Critical commercial assays		
Custom ProcartaPlex Multiplex Panel	Thermo Fisher Scientific	Assay ID: MXU637A
ProcartaPlex Human Basic Kit	Thermo Fisher Scientific	Cat#EPX010-10420-901
LAP Human ProcartaPlex Simplex Kit	Thermo Fisher Scientific	Cat#EPX010-12065-901
Deposited data		
Tumor RNAseq data	Synapse	https://doi.org/10.7303/syn64364142
Normal RNAseq data	Synapse	https://doi.org/10.7303/syn64364380
Experimental models: Cell lines		
MPB Murine Ovarian Cancer cell line	Scott Lowe Lab at MSKCC Paffenholz et al.[29]	Source: https://doi.org/10.1073/pnas.2117754119

(*Continued on next page*)

Continued

REAGENT or RESOURCE	SOURCE	IDENTIFIER
Experimental models: Organisms/strains		
Mouse: C57BL/6 (Taconic) female mice, 6–8 weeks old	Taconic	https://www.taconic.com/products/mouse-rat/standard-strains-and-stocks/black-6-b6ntac
Software and algorithms		
GenomicAlignments package in Bioconductor	Lawrence et al.[21]	https://bioconductor.org/packages/release/bioc/html/GenomicAlignments.html
DESeq2 package	Love et al.[23]	https://bioconductor.org/packages/release/bioc/html/DESeq2.html
HALO Image Analysis Platform	Indica Labs	https://indicalab.com/halo/#
FlowJo	Tree Star Inc.	https://www.flowjo.com/
GraphPad Prism version 9.0	GraphPad	https://www.graphpad.com/
IVIS-SPECTRUM Imaging system	Revvity	https://www.revvity.com/category/in-vivo-imaging

EXPERIMENTAL MODEL AND STUDY PARTICIPANT DETAILS

Human subjects

Patients undergoing PCS for presumed advanced-stage HGSOC were consented to tissue and blood collection and storage under an Institutional Review Board (IRB)-approved protocol at Memorial Sloan Kettering Cancer Center (MSK). Analyses were performed under a separate IRB-approved biospecimen protocol. From June 2018 to March 2022, 51 consecutive patients with OC had tumor and normal tissue and/or peripheral blood collected. Patients were adult female patients over 18 years old with newly diagnosed advanced stage high grade serous ovarian cancer. We excluded patients from additional tissue and plasma analyses if the final pathology of their tumors did not demonstrate HGSOC, if there was incomplete collection of specimens/blood, or if there was low tumor cell content in collected specimens (Figure 1, Tables S1 and S2). Experimental groups: RNA sequencing of fresh frozen tumor/normal specimens (n = 10), serum cytokine analysis (n = 18), immunohistochemical analysis on dtumor/normal formalin fixed paraffin embedded specimens (n = 10). (Table S2).

Murine model and cell lines

Six to 8-week-old C57BL/6 (Taconic) female mice were inoculated peritoneally with 1 million *MYC*-amplified, *TP53*-mutant, *BRCA1*-mutant (MPB) HGSOC cells expressing firefly luciferase, kindly provided by Dr. Scott Lowe's lab at MSK.[20] The MPB cell line is a flexible non-germline-based mouse model that recapitulates the genetic, histological, and molecular features of human HGSOC, which allows us to study genetic and molecular changes during tumorigenesis in immunocompetent mice.[20] The cell line has not been authenticated. Cells were cultured in RPMI medium supplemented with 10% fetal bovine serum and 1% penicillin/streptomycin, and we maintained the cells in a 5% CO_2 atmosphere at 37°C. The cell line was routinely tested for mycoplasma contamination. All experiments with the cells were carried out between passage 3 to 8 (at 75–80% confluence).

METHOD DETAILS

Tissue and plasma collection

Biopsies of tumor tissue and normal peritoneum were collected shortly after initial incision (time point, TP1) and 4 h into the surgery (TP2). Tumor specimens were collected from the same anatomic site to minimize the potential impact of inter-site heterogeneity (Figure 1A). Half of each specimen was immediately snap frozen at the time of collection, and the other half was formalin fixed and paraffin embedded (FFPE). Peripheral blood was collected just prior to incision (sTP1), 4 h after incision (sTP2), and 24 h after laparotomy (sTP3) in an ethylenediaminetetraacetic tube. Within 1 h of collection, the blood sample was centrifuged at 2,000 rpm for 10 min, and then we centrifuged the supernatant at 16,000 rpm for 10 min. Supernatant was removed and frozen at −80°C.

RNA sequencing and gene expression analysis

A pathologist reviewed hematoxylin and eosin–stained sections from the tumor and normal tissue FFPE blocks to define the percentage of neoplastic cells within tumor samples and to verify that normal samples lacked neoplastic cells. Only normal tissues devoid of any neoplastic cells and only tumor samples with >50% neoplastic cells were included. Total RNA was extracted from tumor and matched normal tissues using RNA-Bee and was sequenced using polyA PE50 RNA following validated protocols at MSK's

Integrated Genomics Operation, as previously described.[45,46] In brief, STAR RNA-seq was used to align RNA sequencing reads to the GRCh37 human genome and then GenomicAlignments package in Bioconductor was used to count mapped single-end reads from transcripts.[47–49] To further transform read counts, variance-stabilizing transformation method in the DESeq2 package was utilized for evaluating gene expression and visualization.[50] Differentially expressed genes between TP1 and TP2 were identified using $p < 0.05$ and at least 2-fold change with DESeq2, which uses a negative binomial distribution to model the read counts and account for overdispersion of the count data in RNA-seq. With DESeq2, Wald test was used for hypothesis testing and for estimation of the p value for each gene; the p values were further adjusted to control for false-discovery rate using the Benjamin-Hochberg procedure across the genes. Gene set enrichment analysis was performed for identification of enriched pathways in the Kyoto Encyclopedia of Genes and Genomes database using clusterProfiler according to log2 fold change values.[51]

Immunohistochemistry

Immunohistochemical analyses on tumor and normal FFPE sections were performed to quantify the infiltration with T cells (CD3 [Leica, Clone LN10]) and CD16$^+$ myeloid cells and NK cells (CD16 [Vector, Clone 2H7]).[52–55] For multiplex immunohistochemistry (IHC) image analysis, HALO Image Analysis Platform was utilized (Indica labs, USA) using representative slides and the entire slide was analyzed. Percentage of CD3$^-$and CD16-positive cells out of all cells was calculated for both TP1 and TP2.

Cytokine analysis

Cytokine analysis of blood samples was performed using Luminex Multiplex Assay for 18 patients with available frozen plasma from all three timepoints (sTP1, sTP2, and sTP3). We measured plasma levels of key cytokines (IL-6, IL-1b, IL-8, IL-10, IFNg, TNFa, and TGFb latency-associated peptide [LAP-1]) using human cytokine immunobead panels (Procartaplex multiplex assay, Thermo Fisher Scientific, Waltham, MA) coupled with a multiplex assay (involving xMAP technology, Luminex). Each sample was run in triplicate and average plasma cytokine levels for each plasma timepoint were plotted.

Laparotomy procedure experimental design

On day 5–6 after tumor cell inoculation, mice underwent the intervention of a midline laparotomy (1–2 cm) or no laparotomy. Laparotomy procedure was performed under the approved Institutional Animal Care and Use Committee (IACUC) guidelines and all personnel involved in performing the procedure were appropriately trained.

Description of murine laparotomy procedure

Prior to the laparotomy procedure, mice received 0.5 mg/kg buprenorphine and 2 mg/kg meloxicam subcutaneous injections, and then isoflurane inhaled anesthetic. Following confirmation that a suitable anesthetic plane had been attained (no response to stimulation), we applied sterile eye lubricant to both eyes to prevent corneal drying during the procedure. We shaved the mouse abdomen with electric clippers and cleaned with betadine and 70% isopropyl alcohol. The laparotomy procedure consisted of a 1–2-cm midline vertical incision, including the peritoneum. We inspected the abdomen to ensure no damage to visceral organs and then closed the peritoneum with 5-0 Vicryl sutures and the skin with surgical staples. Post-procedure, we then observed the mouse in a warm environment, and 24 h post-procedure we re-evaluated the mice and administered 2 mg/kg meloxicam subcutaneous injection. Then, 48 and 72 h after the procedure, we also observed the mice to ensure appropriate recovery. The mice that did not undergo laparotomy did not receive any anesthetic or meloxicam injections.

Experimental drug protocol

Mice received intraperitoneal injection of either 400 μg of anti-IL-6 receptor (IL6R) antibody (*InVivo*MAb anti-mouse IL6R, clone 15A7, BioxCell) or 400 μg of control IgG (*InVivo*MAb rat IgG2b isotype control, anti-keyhole limpet hemocyanin, clone LTF-2, BioxCell) 24 h prior to laparotomy/no laparotomy, 24 h post-intervention, and then weekly for 2 weeks.

Tumor burden bioluminescence protocol

The IVIS-SPECTRUM Imaging system was prepared for use according to IACUC guidelines. Animals were placed into the anesthesia induction chamber and anesthetized with 3% isoflurane. When the animals reached a sufficient level of anesthesia, they were intraperitoneally injected with 200 μL of 150 mg/kg luciferin and were moved from the induction chamber to the image acquisition chamber with ongoing anesthesia via nose cone. Luminescence acquisition was performed as described in the instrument's operating manual (PerkinElmer) and average radiance (p/s/cm^2/sr) and total flux (p/s) was obtained for each mouse.

Plasma collection and cytokine analysis

Using a retro-orbital blood collection technique, mouse blood was obtained 24 h pre-procedure and 24 h post-procedure. For cytokine analyses, Luminex Multiplex Assay was used for both timepoints. Plasma levels of key cytokines were measured using mouse cytokine immunobead panels (Procartaplex multiplex assay, Thermo Fisher Scientific, Waltham, MA) coupled with a multiplex assay (involving xMAP technology, Luminex). Each sample was run in duplicate and average plasma cytokine level for each plasma timepoint was obtained.

Flow cytometry

After tumor isolation, the samples were manually diced and were digested using DNAse (Sigma) and Liberase (Roche) for 30 min at 37°C. The digested samples were passed through 70-μm strainers and centrifuged using Percoll 40% to remove debris. Cells were washed in phosphate-buffered saline, incubated in Fc-blocking buffer (PBS with 2.42G2 antibody) for 15 min, and stained using panels of extracellular and intracellular antibodies (Table S3). Stained cells were analyzed using the 5-laser Cytek Aurora spectral flow cytometer (Cytek Biosciences). FlowJo software (Tree Star Inc.) was used for data analysis. The gating strategy for analysis using FlowJo is demonstrated in Figure S1.

QUANTIFICATION AND STATISTICAL ANALYSIS

Data are presented as means and standard error of the mean. For IHC data, Wilcoxon matched-pairs signed-rank test was used to compare TP1 and TP2 percent change of CD3 and CD16 for normal and tumor specimens, separately. For human cytokine data, one-way analysis of variance comparisons between sTP1 and sTP2 or sTP3 were performed. For mouse bioluminescence data, the calculated mean area under the curve of total flux (p/s) for the mice in each cohort (i.e., laparotomy vs. no laparotomy) was used to compare the groups. Statistical comparisons for the cytokine and flow cytometry data were performed using the Mann-Whitney test, and $p < 0.05$ was considered significant. For differential expression analysis, p values were obtained using the Wald test and were further adjusted to correct for the false-discovery rate using the Benjamin-Hochberg procedure. Both $p < 0.05$ and fold change >2 were used to define differentially expressed genes. Statistical analyses were performed using GraphPad Prism version 9.0 (GraphPad Software Inc., http://graphpad.com).

ADDITIONAL RESOURCES

This work is not part of or involving a clinical trial.